Biochimica et Biophysica Acta 1787 (2009) 706–713

Contents lists available at ScienceDirect

Biochimica et Biophysica Acta

journal homepage: www.elsevier.com/locate/bbabio

Review

Bacterial transporters: Charge translocation and mechanism

Constanta Ganea [a], Klaus Fendler [b,*]

[a] Biophysical Department, Faculty of Medicine, Carol Davila University of Medicine and Pharmacy, 8 Eroilor Sanitari Blvd., 050474 Bucharest, Romania
[b] Department of Biophysical Chemistry, Max Planck Institute of Biophysics, Max von Laue Str. 3, D-60438 Frankfurt/Main, Germany

ARTICLE INFO

Article history:
Received 19 December 2008
Received in revised form 2 February 2009
Accepted 2 February 2009
Available online 11 February 2009

Keywords:
Solid supported membrane
Proteoliposome
Bacterial transporter
MelB
PutP
NhaA

ABSTRACT

A comparative review of the electrophysiological characterization of selected secondary active transporters from *Escherichia coli* is presented. In melibiose permease MelB and the Na^+/proline carrier PutP pre-steady-state charge displacements can be assigned to an electrogenic conformational transition associated with the substrate release process. In both transporters cytoplasmic release of the sugar or the amino acid as well as release of the coupling cation are associated with a charge displacement. This suggests a common transport mechanism for both transporters. In the NhaA Na^+/H^+ exchanger charge translocation due to its steady-state transport activity is observed. A new model is proposed for pH regulation of NhaA that is based on coupled Na^+ and H^+ equilibrium binding.

1. Introduction

Secondary active transporters in the bacterial plasma membrane are of fundamental importance for the cell. To name only a few functions, they catalyze the uptake of nutrients, export toxic compounds, translocate macromolecules, regulate cell turgor and create ion gradients essential for the function of other membrane proteins. Recently, bacterial transporters have also become important as prototypic systems in structural biophysics. Because procaryotic membrane proteins are easier to prepare and handle than their eukaryotic counterparts, bacterial homologues of mammalian transporters have been widely used for protein crystallization and structure determination. Therefore, based on the analysis of bacterial transporters principles of the mechanism of transporters in general, prokaryotic as well as eukaryotic, are emerging (see e.g. [1–5]).

Modern techniques for the elucidation of the molecular mechanism of transporters rely on structural determination, computational biophysics and functional analysis. Among the many methods for functional characterization electrophysiology is probably the most universal because it does not require labelled substrates, it is highly sensitive and has a high time resolution. However, apart from a few rare exceptions, bacterial transporters cannot be investigated using voltage clamp or patch clamp methods because of the small size of bacteria and because bacterial transporters are difficult to express in mammalian cells or oocytes. Here, electrophysiology based on solid supported membranes (SSM-based electrophysiology) can be extremely useful [6–10]. It can be used to identify electrogenic partial reactions, to monitor the transport of a charged substrate and determine kinetic parameters of the transporter like rate constants and substrate affinities. In the following we will show the application of SSM-based electrophysiology at the example of three different bacterial transporters.

2. Materials and methods

Preparation of the proteoliposomes: MelB, PutP and NhaA were produced in overexpressing *Escherichia coli* cell lines. They were purified to homogeneity and reconstituted into proteoliposomes of *E. coli* lipid extracts by the biobead detergent extraction method [7,9,11].

SSM-based electrophysiology: The SSM consists of an octadecanethiol/lipid hybrid bilayer on a gold electrode. Proteoliposomes containing the transporter of interest were adsorbed to the SSM. A substrate concentration jump was generated via a rapid solution exchange and the resulting charge displacements were measured via capacitive coupling. For the concentration jump a “non-activating” solution (without substrate) and an “activating solution” (with substrate) were sequentially applied. To prevent artifacts, the non-activating solution contained an inert compound at the same concentration as the substrate. Conditions for the different experiments are given in the figure legends. For the concentration jumps the following nomenclature is used: $\Delta Na = Na^+$ concentration jump; $\Delta mel\Delta Na$ = combined melibiose and Na^+ concentration jump; $\Delta mel(Na)$ = melibiose concentration jump in the presence of Na; and $\Delta Na(mel)$ = Na concentration jump in the presence of melibiose. Analogous

* Corresponding author. Tel.: +49 69 6303 2035; fax: +49 69 6303 2222.
E-mail address: Klaus.Fendler@mpibp-frankfurt.mpg.de (K. Fendler).

0005-2728/$ – see front matter © 2009 Elsevier B.V. All rights reserved.
doi:10.1016/j.bbabio.2009.02.002

expressions are used for other substrate combinations. For a detailed description of the technique see [12].

2.1. The melibiose permease MelB

Sodium/substrate symport (or cotransport) is a widespread mechanism of solute transport across cytoplasmic membranes of pro- and eukaryotic cells. The melibiose permease MelB from *E. coli* is a member of the galactosides-pentoses-hexuronides (GPH) transporter family and links the uphill solute transport of various sugars (α- or β-galactosides, e.g. melibiose) to a downhill electrochemical ion gradient (Na^+, Li^+, or H^+) (for reviews see [13,14]) in a 1:1 stoichiometry [15]. Studies performed by using a variety of biochemical, and biophysical techniques provided information about the structure and function of MelB [15–20]. MelB from *E. coli*, purified and reconstituted in proteoliposomes was the first bacterial co-transporter that could be investigated by an electrophysiological method, namely SSM-based electrophysiology [11].

Electrical signals elicited by concentration jumps of the co-substrates were recorded at a variety of conditions in order to provide information about different partial reactions of the transport cycle like Na^+ and/or melibiose binding to the permease and co-substrate translocation [8,11]. Typical transient currents are shown in Fig. 1A, a Na^+ concentration jump (ΔNa) and a combined Na^+ and melibiose concentration jump (ΔmelΔNa). They show the basic features of the current response: 1) large and fast transient currents decaying mono-exponentially with a time constant $t = 15$ ms were recorded upon a Na^+ or Li^+ concentration jump and 2) transient biphasic currents including both fast ($t = 10$–20 ms) and slow ($t = 300$–400 ms) decay components were found whenever α- or β-galactosides were present [11].

The fast and monophasic transient response was assigned to an ion-induced charge transfer within the transporter. The second charge transfer process, identified from the slow component (350–450 ms) of the biphasic response induced by the simultaneous co-substrates concentration jump, is associated with the inward Na^+-melibiose symport that gives rise to a stationary current which is converted into a transient current decaying slowly with a time constant of ~350 ms by the capacitive recording system [11,21]. This interpretation was supported by the observation that the slow current component of the biphasic response was suppressed upon selective inactivation of the translocation capacity of MelB by *N*-ethyl maleimide (NEM) (Fig. 1B) [11]. NEM is known to bind to only one of the 4 cysteines of the wild-type permease, cysteine 364 [22,23]. It interferes with the transport function of MelB [24,25] but Na^+ dependent sugar binding is not impaired [15].

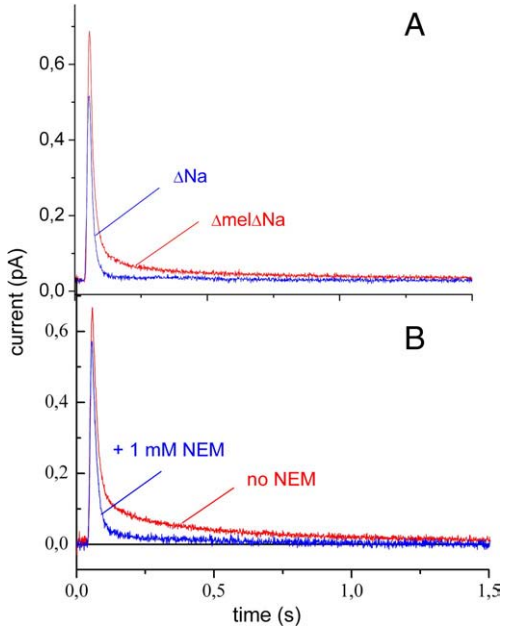

Fig. 1. Melibiose permease MelB. Electrical signals generated by wild-type MelB after different solution exchange protocols. In addition to the sugar and/or cation given below the activating and the non-activating solutions contained 100 mM KP_i at pH 7.0. The data shown in the figure were recorded on the same sample. (A) ΔNa: non-activating solution 50 mM glucose, 10 mM choline chloride (cholineCl), activating solution 50 mM glucose, 10 mM NaCl. ΔmelΔNa: non-activating solution 50 mM glucose, 10 mM cholineCl; activating solution 50 mM melibiose, 10 mM NaCl. In addition both solutions contained 0.1 mM dithiothreitol (DTT). (B) Electrical signals after a simultaneous melibiose and NaCl concentration jump (ΔmelΔNa) before (no NEM) and after (+1 mM NEM) addition of 1 mM NEM: non-activating solution 20 mM glucose, 10 mM cholineCl; activating solution 20 mM melibiose, 10 mM NaCl. All solutions were DTT-free. The experiments were carried out at room temperature (22 °C). Data from [11].

As expected for cation coupled sugar transport, the binding of the cation enhances the affinity of the transporter for the co-transported sugar ($K_{0.5} = 22$ mM in the absence and $K_{0.5} = 3$ mM in the presence of Na^+), and vice versa melibiose enhances the affinity of the transporter for Na^+ ($K_{0.5} = 2.1$ mM in the absence and $K_{0.5} = 0.6$ mM in the presence of melibiose) [11]. The cooperative effect of Na^+ on sugar binding and transport by MelB was already well documented [14,26] but the SSM measurements provided the first evidence for a cooperative influence of the sugar substrate on MelB affinity for the coupling cation. The half saturation constants determined from the electrical measurements were in general in good agreement with those estimated from other biophysical studies using membrane vesicles or proteoliposomes [14,18,27–29].

2.2. A sugar induced electrogenic conformational transition in MelB

While the concentration jumps of Na^+ either in the absence or in the presence of sugar elicited electric signals in line with the anticipated influx of positive charges, it was observed that melibiose, a neutral substrate, both in the presence and in the absence of Na^+ can also trigger an electrical signal upon binding to the permease [8,11]. A tentative interpretation envisioned two possible mechanisms for the electrogenic event triggered by a melibiose concentration jump: the binding of additional Na^+ ions to the protein due to the drastically increased Na^+ affinity after addition of melibiose or a melibiose induced electrogenic conformational change of the protein that displaces either the co-transported H^+ or Na^+ ions or charged residues of the protein. Analysis of the substrate dependencies of the transient currents excludes the first possibility and it could be shown that the observed charge movement is not linked to intraprotein displacement of already bound Na^+ ions [8].

Consequently, the data support a mechanism, in which the molecular events underlying electrogenic Na^+ and melibiose binding are different. Melibiose binding triggers a conformational change that displaces charged intra-protein amino acid side chains or reorients electrical dipoles. Recent experiments performed with an improved SSM configuration allowed to determine the rate constant of $k \sim 250\ s^{-1}$ for this reaction and correlated this charge translocation with a conformational transition of the same rate constant observed in tryptophan fluorescence spectroscopy [30].

2.3. Loop 4-5 plays a central role in conformational changes after sugar binding

The involvement of loop 4-5 in substrate translocation became apparent after the discovery that MelB substrates protect the protein cooperatively against proteolysis of the loop [26]. When the positively charged amino acids of loop 4-5 were individually replaced by a cysteine only R141C, although able to bind the substrates, showed defects in the translocation process [31]. By using cysteine less MelB as genetic background [23,31], the effects of individual cysteine replacements of two electrically charged residues of the loop 4-5, the positively charged R141 and the negatively charged E142, were further analyzed by combining kinetic, electrophysiological, and fluorescence spectros-

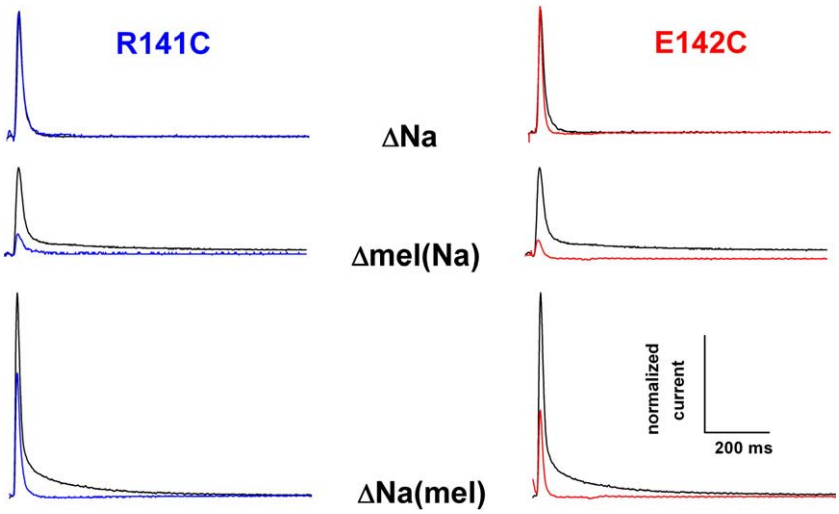

Fig. 2. Melibiose permease MelB. Comparison of the transient currents recorded with R141C, E142C, and cysteine less MelB. Three different substrate concentration jumps were imposed. The activating and non-activating solutions contained 0.1 M KP_i, 0.1 mM DTT, pH 7, and sugar and/or cation as follows: ΔNa: non-activating solution: 50 mM glucose, 10 mM KCl, activating solution: 50 mM glucose, 10 mM NaCl. Δmel(Na): non-activating solution: 50 mM glucose, 10 mM NaCl, activating solution: 50 mM melibiose, 10 mM NaCl. ΔNa(mel): non-activating solution: 50 mM melibiose, 10 mM KCl, activating solution: 50 mM melibiose, 10 mM NaCl. The upper trace in each signal-pair was recorded from the cysteine less mutant and the lower trace from R141C (left part of the figure) or E142C (right part of the figure). Data were normalized to the absolute peak current of the respective ΔNa signal. The experiments were carried out at room temperature (22 °C). Data from [32].

copy approaches [32]. When the charges are removed in R141C and E142C MelB the permease retains still the capacity to bind the co-substrates while transport is inhibited [32]. Consequently, the slow component of the transient currents observed in SSM-based electrophysiology, which was assigned to transport, completely disappears in the case of R141C or is largely suppressed in E142C (Fig. 2, ΔNa (mel)). Reintroducing a positive charge by reacting R141C with the SH-reagent $MTSEA^+$ partially restores active substrate transport as previously shown in transport assays [31], whereas the negatively charged sulfhydryl reagent $MTSES^-$ had no effect in the E142C mutant possibly due to accessibility limitation [32].

Previous studies demonstrated a Na^+-dependent, sugar-induced increase in the tryptophan fluorescence recorded in the native or cysteine less transporter, that has been attributed to cooperative conformational changes either associated to or following binding of the substrates [27,28,33]. The kinetic properties and in particular the rate constant of this conformational change are identical to that of the sugar induced electrogenic reaction [30] and are therefore most probably correlated. The sugar-induced increase of the tryptophan fluorescence is absent in the mutants R141C and E142C (Fig. 3) as are the transient currents (Fig. 2).This led to the conclusion that the electrogenic conformational change after melibiose binding is disturbed in R141C and E142C permeases [32].

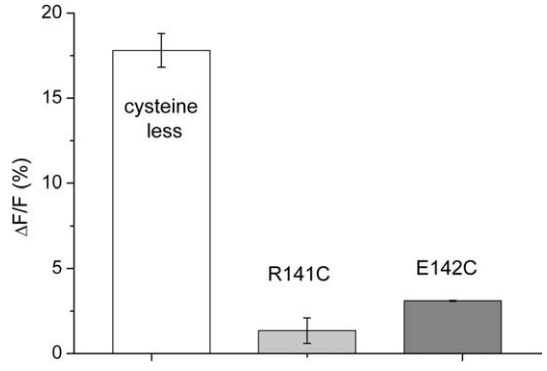

Fig. 3. Melibiose permease MelB. Na^+-dependent tryptophan fluorescence change after melibiose addition to cysteine less, R141C, and E142C MelB. Samples in 0.1 M KP_i, pH 7 medium, were excited at 297 nm (bandpass 5 nm). The fluorescence emission spectra (310–380 nm, bandpass 5 nm) were recorded before and after addition of 10 mM Na^+, and 30 mM melibiose. The fluorescence intensity (F) was integrated between 310 and 380 nm and the relative fluorescence change (ΔF) was calculated. Mean value of three experiments with SEM are given. The fluorescence change after Na^+ and melibiose addition was significantly smaller in E142C and R141C, indicating absence of the sugar induced conformational transition. Data from [32].

It is interesting to note that a different phenotype of inhibition is observed in R141C and E142C as compared to NEM-inhibited wild-type MelB. At first glance both phenotypes seem to be the same, namely substrate binding is still intact while transport is inhibited. However, an important distinction shows up in the activities related to the sugar induced conformational transition. While this reaction is still observed in tryptophane fluorescence [15,18] and SSM-based electrophysiology (Fig. 1B) of the NEM-inhibited enzyme it was absent in the mutants, suggesting that the partial reactions inhibited by NEM and by the mutations at positions 141 and 142 are different. This observation suggested a model according to which the substrate translocation in MelB is a two-step process consisting of an electrogenic conformational transition inhibited in R141C and E142C MelB (C_{cyt}Namel ↔ C′Namel in Fig. 4) followed by a second NEM-inhibitable reaction [32] (C′Namel ↔ C_{peri}Namel in Fig. 4). It was suggested that the state C′Namel is an occluded state [32] acting as an intermediate between the inward- to the outward-facing conformations and that the residues R141 and E142 in the local domain of loop 4-5 are essential for the formation of this intermediate.

2.4. The Na^+/proline transporter PutP

PutP from *E. coli* is a member of the Na^+/substrate symporter (SSS) family comprising far over hundred similar proteins from archaea, bacteria, yeast, insects, and mammals [34]. It catalyzes the coupled translocation of proline and Na^+ with a stoichiometry of 1:1. The coupling ion can also be Li^+. A crystal structure for PutP is not available yet. However, the recently determined structure of a close relative in the same family, the Na^+/glucose cotransporter SGLT1 [35], may provide insight into the specific structural features of this class of transporters. Transport and electrophysiological measurements have provided information about pre-steady-state and steady-state kinetics of members of the SSS family. For SGLT1, a 6-state, ordered kinetic model with mirror symmetry, in which Na^+ binds before sugar, has been used to simulate transport function [36–38]. Similarly, an ordered binding mechanism with binding of Na^+ before proline was proposed for PutP [32].

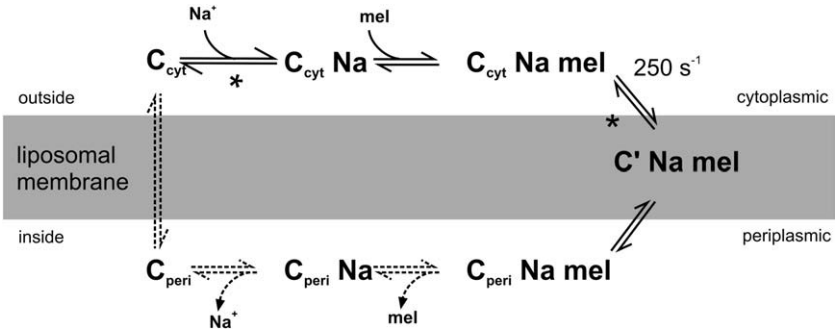

Fig. 4. Melibiose permease MelB. Extended 6-state kinetic model for the backward running MelB transporter. C_{cyt} corresponds to the carrier set with its cytoplasmic binding sites exposed to the solution outside of the proteoliposomes, C_{peri} to the carrier with its periplasmic binding sites exposed to the inside of the liposomes. Na^+ and melibiose binding and release are sequential. Loaded carrier reorientation is proposed to proceed in two steps (C_{cyt}Namel ↔ C′Namel and C′Namel ↔ C_{peri}Namel). The asterisk indicates an electrogenic step. Reactions not contributing to the initial rapid charge displacement are marked by dashed lines.

SSM-based electrophysiology allowed for the first time a direct electrical analysis of PutP [7]. In these experiments the transporter is inside out oriented in the liposomal membrane [39]. Therefore, the observed transport activity corresponds physiologically to the backward running carrier. Application of concentration jumps of the two substrates in different combinations to activate PutP produced transient currents in all cases (Fig. 5). These experiments demonstrate that the activity of the transporter is associated with a charge displacement. Extensive control measurements support this conclusion [7]. Additional evidence comes from the behavior of the electrical signals, which agrees with the known properties of the PutP transporter: for example, cooperativity of the two co-substrates and substrate affinities, which are in reasonable agreement with previous binding studies [7].

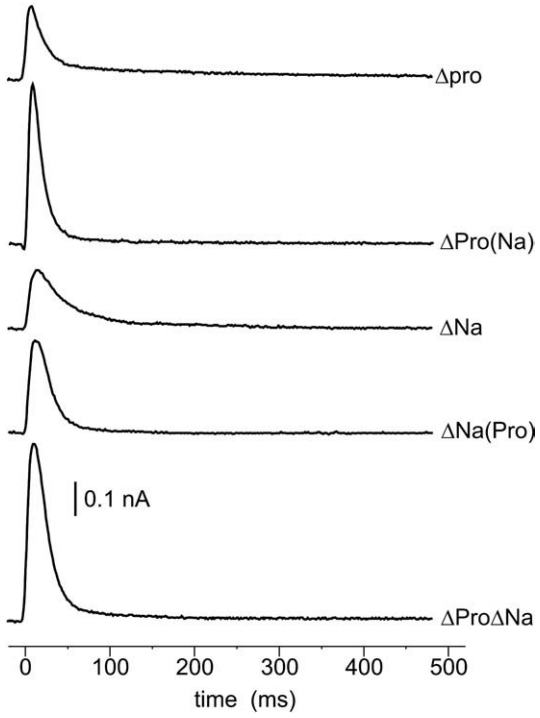

Fig. 5. Proline carrier PutP. Transient currents after different solution exchange protocols. In addition to the amino acid and/or cation given below the activating and non-activating solutions contained 100 mM KP_i and 0.1 mM DTT at pH 7.0. All the data shown in the figure were recorded on the same sample. Δpro: activating solution 100 mM proline; non-activating solution 100 mM alanine. Δpro(Na): activating solution 100 mM proline, 40 mM NaCl; non-activating solution 100 mM alanine, 40 mM NaCl. ΔNa: activating solution 40 mM NaCl; non-activating solution 40 mM KCl. ΔNa (pro): activating solution 40 mM NaCl, 100 mM proline; non-activating solution 40 mM KCl, 100 mM proline. ΔproΔNa: activating solution 100 mM proline, 40 mM NaCl; non-activating solution 100 mM alanine, 40 mM KCl. Figure reproduced with permission from [7].

Since rise and decay of the signals are rapid (8.5–21 ms) compared to the turnover of the enzyme (~1 s^{-1}) [39], the electrogenic reaction has to be a fast step (k>50 s^{-1}) early in the reaction cycle preceding the rate limiting step. The fact that also in the absence of the respective co-substrate (i.e. in the presence of Na^+ or melibiose alone) the transient currents are observed suggests that it is an electrogenic substrate binding reaction preceding the general reorientation of the carrier [7].

The translocated charge measured for the different solution exchange protocols provides information about the electrogenic substrate binding process. First, each substrate can bind individually without the need for the presence of the other. However, in line with the cooperative nature of the transport process of PutP, a strong proline affinity enhancement was found when Na^+ was present. The translocated charge is approximately the same for Na^+ and proline binding whether the respective co-substrate is present or not (Fig. 6). It doubles, however, when both substrates bind simultaneously. This supports the concept that either substrate can bind individually to the transporter and that the charge displacement associated with the binding process is approximately the same.

2.5. Proline binding is a two step process

Analysis of the proline affinity of PutP in the presence of Na^+ showed a complex behavior: A high affinity (41 μM) was determined when the integrated charge was considered and a low affinity (0.87 mM) when the peak current was used [7]. At the same time [^{14}C]-Proline binding experiments with cytoplasmic membrane

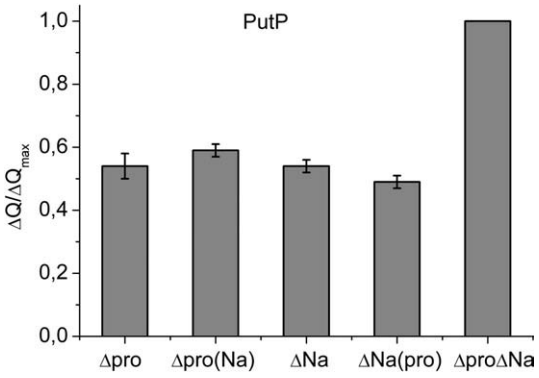

Fig. 6. Proline carrier PutP. Relative displaced charge ($\Delta Q/\Delta Q_{max}$) during the different solution exchange protocols. Mean values of 4 independent experiments and their standard errors (SEM) are shown. Conditions as in Fig. 5. The integrated charge ΔQ was determined by integrating the signals in the time range $0 \le t \le 100$ ms and normalized to its maximal value (ΔQ_{max}) obtained in the ΔproΔNa experiment. Data from [7].

vesicles yielded an affinity constant of 8 μM in the presence of $^{22}Na^+$ [40]. The general picture that emerges is that of a high binding affinity (corresponding to bound [^{14}C]-Proline or integrated charge) while the rate of the binding process (corresponding to the peak current) is characterized by a low affinity constant. A straightforward explanation for this is provided by a kinetic model that consists of a low affinity ($K_D = 0.9$ mM) electroneutral binding reaction followed by a nearly irreversible electrogenic conformational transition that displaces the substrate into the protein [7]. When the integrated charge is considered, the nearly irreversible conformational transition increases the apparent affinity to ~40 μM.

2.6. A mechanism for substrate binding in PutP

Surprisingly, the zwitterion proline that carries no net charge generates a charge displacement also in the absence of Na^+. This can only be explained by a proline induced electrogenic conformational transition displacing charged residues of the protein. The electrogenic nature of the proline binding process supplies a straightforward explanation for the fact that a negative electrical potential inside the liposomes is required for high affinity proline uptake ([41], A. Hackmann, M. Nietschke, and H. Jung, unpublished information). The results obtained so far rule out a mechanism of transporter function where the two substrates bind in "shallow" binding sites and are only displaced into the protein when both are present. The model shown in Fig. 7 accounts for the fact that Na^+ and proline both can bind to the PutP carrier individually. For both substrates, Na^+ and proline, a saturable binding behavior is found in the presence and absence of the other [7]. Using the parameters determined in Ref. [7], binding constants can be inserted into the model as shown in Fig. 7. The proline affinity at the cytoplasmic binding side of PutP in the presence of Na^+ is indeed much lower than previously thought. This model correctly predicts the concentration dependence of the electrical experiments [7]. Also the size of the electrical signals can be accounted for in the model by assigning an approximately equal charge displacement to the binding reactions of the individual substrates (see Fig. 6). In the case of the ΔproΔNa experiments, two subsequent binding reactions are passed through, resulting in a twice as big charge translocation which approximates the experimental results (Fig. 6).

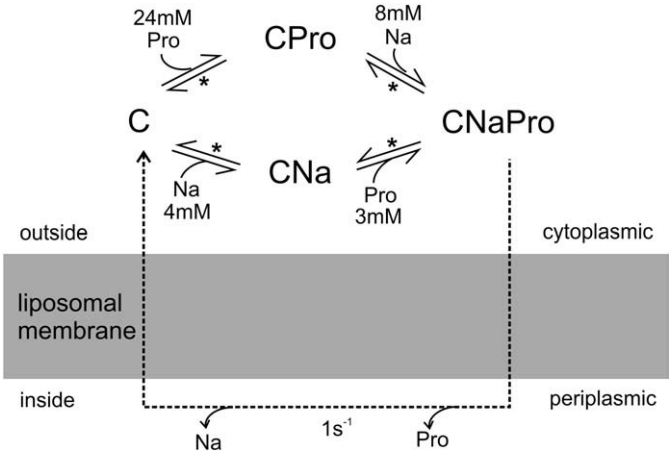

Fig. 7. Proline carrier PutP. Simplified kinetic model for intracellular proline and Na^+ binding and dissociation. The asterisk denotes an electrogenic reaction. Affinities given as determined in [7]. Note that the two substrates can bind individually. The presence of the co-substrate only enhances affinity in the case of proline binding. The dashed line indicates periplasmic release of the substrates and return of the empty carrier leading to steady state turnover. This part of the reaction cycle does not contribute to the initial rapid charge translocation.

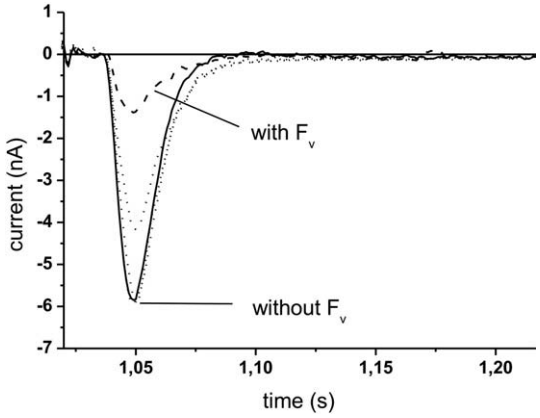

Fig. 8. Na^+/H^+ exchanger NhaA. Inhibitory effect of the monoclonal antibody fragment F_v-2C5. Transient currents generated by a 10 mM Na^+ concentration jump at $t = 1.0$ s. Signals recorded before (solid line without F_v) and after incubation (10 min) of the proteoliposomes adsorbed to the SSM with 25 μl containing 6.9 mg/ml F_v-2C5 (dashed line with F_v). The signal recovered after rinsing with antibody free solution (dotted lines). The buffer solution contained 10 mM KCl, 1 mM DTT, 100 mM Tris, 100 mM Mops, 100 mM Hepes, pH 8.0 (KOH). The activating and the non-activating solution contained in addition 10 mM NaCl or 10 mM KCl respectively. Figure reproduced with permission from [9].

2.7. The NhaA Na^+/H^+ exchanger

Sodium proton antiporters [42] are ubiquitous membrane proteins found in the cytoplasmic and organelle membranes of cells of many different origins. NhaA (a member of the NhaA family of Na^+, K^+/H^+ exchangers from animals, plants, fungi and bacteria, [43]) is an electrogenic antiporter (stoichiometry 2 H^+ for 1 Na^+ [44]) of *E. coli* that is indispensable for adaptation to high salinity, for challenging Li^+ toxicity, and for growth at alkaline pH (in the presence of Na^+) [45–48]. One of the most interesting characteristics of NhaA is its dramatic dependence on pH, a property it shares with both prokaryotic [49] and eukaryotic antiporters [50–52]. The activity of NhaA changes over three orders of magnitude between pH 6.5 to pH 8.5 [47,53]. Among the three bacterial transporters discussed in this review, NhaA is the only one where a structure with atomic resolution is available [3]. The structure revealed an interesting broken helix motive that has been interpreted as a crucial structural element conveying mobility to the transporter [3]. This motive was later found also in other transporters [35,54].

Transient currents were measured after a rapid solution exchange from a Na^+ (or Li^+) free to a Na^+ or (Li^+) containing solution using NhaA proteoliposomes and SSM-based electrophysiology. The negative currents in Fig. 8 represent translocation of positive charge out of the proteoliposomes in agreement with the stoichiometry of NhaA. The carrier is reconstituted with a high efficiency in right side out orientation [9]. Therefore, the observed electric activity of NhaA using SSM-based electrophysiology allowed the study of the properties of the passive downhill uptake mode of the carrier. Physiologically this is a reverse mode of the carrier, which in bacteria is mainly involved in H^+ driven Na^+ extrusion. These currents were selectively inhibited by the NhaA specific monoclonal antibody fragment F_v-2C5 (Fig. 8) binding to a loop exposed to the periplasmic side of the membrane [55] and by the specific inhibitor 2-aminoperimidine [9]. Hence this measurement represented the first direct evidence of electric current mediated by NhaA.

2.8. The transient electrical signals represent stationary turnover of the NhaA exchanger in the passive downhill uptake mode

An interesting property of NhaA is its high turnover. Values up to 1000 s^{-1} at pH 8.0 [53] have been reported. Consequently, the transient signals of NhaA were up to 10 times larger than those

obtained with other transporters [7,11]. In addition, it was observed that the decay time constant of the transient currents decreases with increasing carrier density in the liposomal membrane [9]. This indicates that rather than reflecting the kinetic properties of the NhaA exchanger the decay of the current is brought about by charging of the liposomes. It was concluded that the carrier relaxes rapidly into steady state at pH 8.5 as well as at pH 7.0 when turnover is low [9]. The peak current, therefore, represents stationary turnover of the NhaA Na^+/H^+ exchanger in contrast to MelB and PutP which show a pre-steady-state behavior.

2.9. pH regulation and cation dependence of NhaA

NhaA is strongly regulated by pH. As assessed by measuring passive ^{22}Na efflux, turnover of the enzyme increases by a factor of more than 1000 when raising the pH from pH 6.5 to pH 8.5 [53]. The passive efflux experiments performed with proteoliposomes in the absence of a membrane potential and a pH gradient represent the exact reverse mode compared to the passive downhill uptake mode probed by SSM-based electrophysiology. Interestingly, in the latter the antiporter showed significantly different properties. As shown in Fig. 9, the apparent K_m for Na^+ is drastically increased at neutral pH while in the efflux mode pH regulation changes mainly turnover [9]. In passive downhill uptake mode, K_m as well as turnover V_{max} both increase by

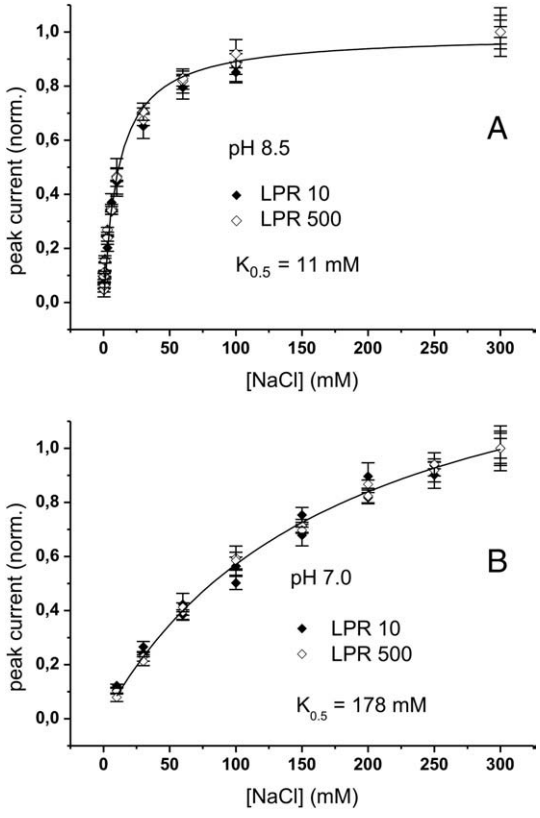

Fig. 9. Na^+/H^+ exchanger NhaA. Concentration dependence of the transient currents after a Na^+ concentration jump. Transient currents were measured at pH 8.5 and pH 7.0. For comparison proteoliposomes with a lipid to protein ratio (LPR) of 10 (solid symbols) and 500 (open symbols) were used. The peak currents were normalized to V_{max}. The values given in the figure are average values of 3 subsequent recordings, error bars represent SEM. Note that the concentration dependence is independent of LPR indicating that charging of the liposomes does not reduce the peak current at high substrate concentrations. (A) Peak currents measured at pH 8.5. Activating solution: x mM NaCl, $(300-x)$ mM KCl. Nonactivating solution: 300 mM KCl. In addition the buffers contained 5 mM $MgCl_2$, 25 mM HEPES, 25 mM Tris, pH 8.5(KOH). (B) Peak currents measured at pH 7.0. Activating solution: x mM NaCl, $(300-x)$ mM KCl. Nonactivating solution: 300 mM KCl. In addition the buffers contained 5 mM $MgCl_2$, 25 mM HEPES, 25 mM Tris, pH 7.0 (HCl). Figure reproduced with permission from [9].

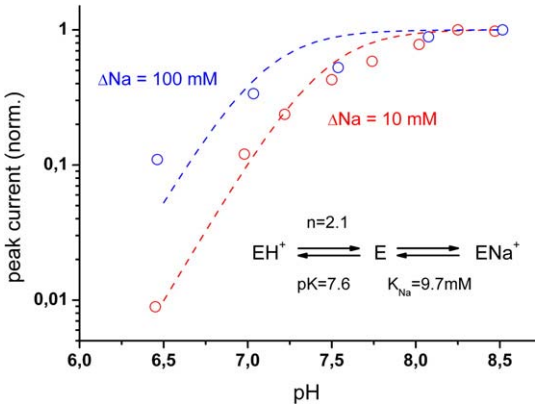

Fig. 10. Na^+/H^+ exchanger NhaA. pH regulation in the passive downhill uptake mode. Peak currents at different pH after a 10 mM (red circles) or a 100 mM (blue circles) Na^+ concentration jump. The data are normalized to the current at pH 8.5. The kinetic model shown in the figure was used to calculate the normalized NhaA activity as a function of pH and Na^+ concentration (dashed lines). Data from [9].

approximately a factor of 10 when changing from neutral (pH 6.5–7.0) to basic (pH 8.5) conditions (Fig. 10). Therefore, it was suggested that at acidic pH a pH signal at the pH "sensor" triggers a structural change of NhaA that slows down the rate limiting step and at the same time increases the apparent K_m for Na^+ at the periplasmic side of the transporter [9]. On the other hand, new structural evidence suggested that instead of a kinetic effect on the rate limiting step, acidification drives the enzyme into a down-regulated conformation that does not contribute to transport [3,56].

We have, therefore, reexamined the data on the basis of a kinetic model inspired by the structural model for pH regulation put forward by [3]. It is assumed that the protonated form of the enzyme EH^+ is the downregulated conformation and that the Na^+ bound form ENa^+ is the active conformation (see Fig. 10). Enzyme activity is, therefore, proportional to the concentration of ENa^+ which can be calculated as a function of H^+ and Na^+ equilibrium binding according to the kinetic model shown in Fig. 10:

$$\frac{ENa^+}{E_{tot}} = \frac{c_{Na}}{c_{Na} + K_{Na}(pH)}.$$

E_{tot} is the total enzyme concentration and $K_{Na}(pH)$ is a pH dependent apparent dissociation constant for Na^+ given by:

$$K_{Na}(pH) = K_{Na}\left[1 + 10^{n(pK-pH)}\right].$$

Here Na^+ binding is described by the Na^+ dissociation constant K_{Na}. Cooperative H^+ binding is assumed with pK and a Hill coefficient n. The parameters pK, K_{Na} and n were optimized to match the experimental results in Figs. 9 and 10. An optimal fit to the data was obtained with $pK = 7.6$, $n = 2.1$ and $K_{Na} = 9.7$ mM yielding the apparent Na^+ dissociation constants $K_{Na}(8.5) = 9.8$ mM, $K_{Na}(7.0) = 186$ mM and the pH dependence as shown in Fig. 10. The good agreement of this functional model with the experimental data adds confidence to the pH regulatory mechanism proposed from the structural study [3]. Note that in this model the binding properties of the Na^+ binding site are independent of pH and the modified K_m for Na^+ at different pH is brought about by the coupled binding equilibria of H^+ and Na^+.

3. Concluding remarks

3.1. SSM-based electrophysiology

SSM-based electrophysiology has been proven to be a valuable complement to the electrophysiological toolbox. Its particular advantage becomes apparent when membrane proteins from bacteria and

eukaryotic intracellular compartments, like the sarcoplasmic reticulum or vesicles from parietal cells, have to be studied. Because of their small size, these structures are in general not accessible for standard electrophysiology, like the two electrode voltage clamp or patch clamp techniques. Purified and reconstituted into liposomes bacterial transporters can be investigated without complications arising from interactions with other components of the membrane or the intracellular medium.

The compound membrane is a well suited substrate for the investigation of transport proteins; it provides both a lipidic phase and aqueous spaces on both sides of the membrane for the protein. A further advantage of adsorbing membrane fragments or proteoliposomes to a planar membrane is the much simpler and more effective procedure compared to incorporation of the protein in the planar membrane, leading to a superior signal to noise ratio and time resolution of the electrical measurement. A problem for reconstituted systems is orientation. Random orientation of the transporter in the liposomal membrane would not be optimal in view of an analysis in terms of structure function relationship. Fortunately, many transporters insert into the liposomes in nearly perfect unidirectional orientation, e.g. PutP [39] and MelB [39] in inside out and LacY [57] and NhaA [9,57] in right side out orientation (for a review of oriented reconstitution see [58]).

3.2. NhaA compared to MelB and PutP

In all three cases discussed in this review, the Na^+ or substrate concentration jumps applied to the transporters induce a reverse mode in the physiological sense. However, the electrophysiological experiments on NhaA fall into a different category: 1) NhaA is right side out oriented while MelB and PutP are inside out oriented in the proteoliposomes. Therefore, the kinetic parameters determined for NhaA correspond to the periplasmic side of the protein while those for MelB and PutP reflect the cytoplasmic side. 2) The observed NhaA currents represent steady state turnover of the enzyme. The currents obtained with MelB and PutP, on the other hand, are dominated by pre-steady-state charge displacements. This indicates that in NhaA the electrogenic step occurs late (compared to substrate binding) in the reaction cycle in contrast to MelB and PutP.

3.3. Electrogenic substrate release in MelB and PutP

Comparison of the electrogenic characteristics of MelB and PutP reveals a number or surprising similarities. In particular two features are of importance for the transport mechanism: 1) The two substrates, Na^+ and sugar/amino acid bind individually though in a cooperative manner to the transporter and 2) binding of both substrates induces a rapid charge translocation of comparable magnitude. Since both transporters are inside out oriented in the liposome membrane the electrophysiological experiments probe reactions corresponding to substrate release in terms of their physiological transport mode. For the interpretation of the kinetic data not only the orientation of the transporters in the membrane, but also their initial configuration before the substrate concentration jump is of importance. The question is whether in the absence of substrate the binding sites are open to the cytoplasmic (inward-facing) or to the periplasmic side (outward-facing)? The low resolution structure of MelB suggested an inward-facing topology [19]. For PutP structural information is not yet available. The crystal structure of vSGLT1, a close relative of PutP and the first member of the SSS family crystallized so far revealed an inward-facing conformation [35]. This may be taken as an indication that the lowest free energy state of these transporters is the inward-facing conformation. Consequently, because of their inside out orientation, the cytoplasmic substrate binding sites are available for substrate binding in our electrophysiological experiments (i.e. in the reverse transport mode). This is supported by our electrophysiological experiments which show rapid electrogenic substrate binding ($\sim 250\ s^{-1}$, [30]) without an apparent lag phase due to preceding electroneutral reactions. Incidentally, the functional homology between MelB and PutP parallels a functional similarity of MelB and SGLT1 [59], the latter a member of the SSS family like PutP.

As mentioned above, the charge displacements detected in our electrophysiological study of MelB and PutP represent substrate release in the physiological transport mode. The data show that this process is preceded by an electrogenic conformational transition, possibly a deocclusion reaction as suggested before [32]. No decisive information is available yet about the electrogenicity of the periplasmic substrate binding steps. Preliminary experiments with LacY (unpublished observation) seem to indicate, that much less charge is translocated during these reactions. In conclusion, the electrophysiological studies suggest a rather asymmetrical functional model for the Na^+/solute transporters. In a recent structural study inward- and outward-facing conformations of the Na^+/galactose transporter vSGLT1 were presented [35]. There, the inward-facing conformation has a narrow access pathway to the substrate binding sites while in the outward-facing conformation the pathway is wide. This may represent a structural rationale for the functional asymmetry observed in our studies.

Acknowledgments

We thank Etana Padan, Gerard Leblanc and Juan-J. Garcia-Celma for critical reading of the manuscript. Ernst Bamberg is gratefully acknowledged for helpful discussions and support. This work has been supported by the Deutsche Forschungsgemeinschaft SFB 472.

References

[1] I.T. Arkin, H. Xu, M.O. Jensen, E. Arbely, E.R. Bennett, K.J. Bowers, E. Chow, R.O. Dror, M.P. Eastwood, R. Flitman-Tene, B.A. Gregersen, J.L. Klepeis, I. Kolossvary, Y. Shan, D.E. Shaw, Mechanism of Na^+/H^+ antiporting, Science 317 (2007) 799–803.
[2] O. Boudker, R.M. Ryan, D. Yernool, K. Shimamoto, E. Gouaux, Coupling substrate and ion binding to extracellular gate of a sodium-dependent aspartate transporter, Nature 445 (2007) 387–393.
[3] C. Hunte, E. Screpanti, M. Venturi, A. Rimon, E. Padan, H. Michel, Structure of a Na^+/H^+ antiporter and insights into mechanism of action and regulation by pH, Nature 435 (2005) 1197–1202.
[4] E. Padan, The enlightening encounter between structure and function in the NhaA Na^+–H^+ antiporter, Trends Biochem. Sci. 33 (2008) 435–443.
[5] H. Jayaram, A. Accardi, F. Wu, C. Williams, C. Miller, Ion permeation through a Cl-selective channel designed from a CLC Cl^-/H^+ exchanger, Proc. Natl. Acad. Sci. U. S. A. 105 (2008) 11194–11199.
[6] C. Burzik, G. Kaim, P. Dimroth, E. Bamberg, K. Fendler, Charge displacements during ATP-hydrolysis and synthesis of the Na^+-transporting FoF1-ATPase of *Ilyobacter tartaricus*, Biophys. J. 85 (2003) 2044–2054.
[7] A. Zhou, A. Wozniak, K. Meyer-Lipp, M. Nietschke, H. Jung, K. Fendler, Charge translocation during cosubstrate binding in the Na^+/proline transporter of *E. coli*, J. Membr. Biol. 343 (2004) 931–942.
[8] K. Meyer-Lipp, C. Ganea, T. Pourcher, G. Leblanc, K. Fendler, Sugar binding induced charge translocation in the melibiose permease from *Escherichia coli*, Biochemistry 43 (2004) 12606–12613.
[9] D. Zuber, R. Krause, M. Venturi, E. Padan, E. Bamberg, K. Fendler, Kinetics of charge translocation in the passive downhill uptake mode of the Na^+/H^+ antiporter NhaA of *Escherichia coli*, Biochim. Biophys. Acta 1709 (2005) 240–250.
[10] S. Raunser, M. Appel, C. Ganea, U. Geldmacher-Kaufer, K. Fendler, W. Kuhlbrandt, Structure and function of prokaryotic glutamate transporters from *Escherichia coli* and *Pyrococcus horikoshii*, Biochemistry 45 (2006) 12796–12805.
[11] C. Ganea, T. Pourcher, G. Leblanc, K. Fendler, Evidence for intraprotein charge transfer during the transport activity of the melibiose permease from *Escherichia coli*, Biochemistry 40 (2001) 13744–13752.
[12] P. Schulz, J.J. Garcia-Celma, K. Fendler, SSM-based electrophysiology, Methods 46 (2008) 97–103.
[13] B. Poolman, J. Knol, C. Vanderdoes, P.J.F. Henderson, W.J. Liang, G. Leblanc, T. Pourcher, I. Mus-Veteau, Cation and sugar selectivity determinants in a novel family of transport proteins, Mol. Microbiol. 19 (1996) 911–922.
[14] T. Pourcher, M. Bassilana, H.K. Sarkar, H.R. Kaback, G. Leblanc, The melibiose/Na^+ symporter of *Escherichia coli*: kinetic and molecular properties, Philos. Trans. R. Soc. Lond., B Biol. Sci. 326 (1990) 411–423.
[15] E. Damiano-Forano, M. Bassilana, G. Leblanc, Sugar binding properties of the melibiose permease in *Escherichia coli* membrane vesicles. Effects of Na^+ and H^+ concentrations, J. Biol. Chem. 261 (1986) 6893–6899.

[16] M. Bassilana, T. Pourcher, G. Leblanc, Melibiose permease of *Escherichia coli*. Characteristics of co-substrates release during facilitated diffusion reactions, J. Biol. Chem. 263 (1988) 9663–9667.
[17] X. Leon, V.A. Lorenz-Fonfria, R. Lemonnier, G. Leblanc, E. Padros, Substrate-induced conformational changes of melibiose permease from *Escherichia coli* studied by infrared difference spectroscopy, Biochemistry 44 (2005) 3506–3514.
[18] C. Maehrel, E. Cordat, I. Mus-Veteau, G. Leblanc, Structural studies of the melibiose permease of *Escherichia coli* by fluorescence resonance energy transfer — I. Evidence for ion-induced conformational change, J. Biol. Chem. 273 (1998) 33192–33197.
[19] P. Purhonen, A.K. Lundback, R. Lemonnier, G. Leblanc, H. Hebert, Three-dimensional structure of the sugar symporter melibiose permease from cryo-electron microscopy, J. Struct. Biol. 152 (2005) 76–83.
[20] D.M. Wilson, T.H. Wilson, Asp-51 and Asp-120 are important for the transport function of the *Escherichia coli* melibiose carrier, J. Bacteriol. 174 (1992) 3083–3086.
[21] K. Fendler, S. Jaruschewski, A. Hobbs, W. Albers, J.P. Froehlich, Pre-steady-state charge translocation in NaK-ATPase from eel electric organ, J. Gen. Physiol. 102 (1993) 631–666.
[22] M.C. Botfield, T.H. Wilson, Mutations that simultaneously alter both sugar and cation specificity in the melibiose carrier of *Escherichia coli*, J. Biol. Chem. 263 (1988) 12909–12915.
[23] A.C. Weissborn, M.C. Botfield, M. Kuroda, T. Tsuchiya, T.H. Wilson, The construction of a cysteine-less melibiose carrier from *E. Coli*, Biochim. Biophys. Acta 1329 (1997) 237–244.
[24] M. Bassilana, T. Pourcher, G. Leblanc, Facilitated diffusion properties of melibiose permease in *Escherichia coli* membrane vesicles. Release of co-substrates is rate limiting for permease cycling, J. Biol. Chem. 262 (1987) 16865–16870.
[25] J. Lopilato, T. Tsuchiya, T.H. Wilson, Role of Na^+ and Li^+ in thiomethylgalactoside transport by the melibiose transport system of *Escherichia coli*, J. Bacteriol. 134 (1978) 147–156.
[26] C. Gwizdek, G. Leblanc, M. Bassilana, Proteolytic mapping and substrate protection of the *Escherichia coli* melibiose permease, Biochemistry 36 (1997) 8522–8529.
[27] I. Mus-Veteau, G. Leblanc, Melibiose permease of *Escherichia coli* — structural organization of cosubstrate binding sites as deduced from tryptophan fluorescence analyses, Biochemistry 35 (1996) 12053–12060.
[28] I. Mus-Veteau, T. Pourcher, G. Leblanc, Melibiose permease of *Escherichia coli*: substrate-induced conformational changes monitored by tryptophan fluorescence spectroscopy, Biochemistry 34 (1995) 6775–6783.
[29] M.L. Zani, T. Pourcher, G. Leblanc, Mutation of polar and charged residues in the hydrophobic NH2-terminal domains of the melibiose permease of *Escherichia coli*, J. Biol. Chem. 269 (1994) 24883–24889.
[30] J.J. Garcia-Celma, B. Dueck, M. Stein, M. Schlueter, K. Meyer-Lipp, G. Leblanc, K. Fendler, Rapid activation of the melibiose permease MelB immobilized on a solid-supported membrane, Langmuir 24 (2008) 8119–8126.
[31] M. Abdel-Dayem, C. Basquin, T. Pourcher, E. Cordat, G. Leblanc, Cytoplasmic loop connecting helices IV and V of the melibiose permease from *Escherichia coli* is involved in the process of Na^+-coupled sugar translocation, J. Biol. Chem. 278 (2003) 1518–1524.
[32] K. Meyer-Lipp, N. Sery, C. Ganea, C. Basquin, K. Fendler, G. Leblanc, The inner interhelix loop 4-5 of the melibiose permease from *Escherichia coli* takes part in conformational changes after sugar binding, J. Biol. Chem. 281 (2006) 25882–25892.
[33] G. Leblanc, M. Bassilana, E. Damiano, Na^+/H^+ Exchange in Bacteria and Organelles, CRC Press, Boca Raton, FL, 1988.
[34] H. Jung, Minireview. The sodium/substrate symporter family: structural and functional features, FEBS Lett. 529 (2002) 73–77.
[35] S. Faham, A. Watanabe, G.M. Besserer, D. Cascio, A. Specht, B.A. Hirayama, E.M. Wright, J. Abramson, The crystal structure of a sodium galactose transporter reveals mechanistic insights into Na^+/sugar symport, Science 321 (2008) 810–814.
[36] S. Falk, A. Guay, C. Chenu, S.D. Patil, A. Berteloot, Reduction of an eight-state mechanism of cotransport to a six-state model using a new computer program, Biophys. J. 74 (1998) 816–830.
[37] M. Panayotova-Heiermann, D.D. Loo, E.M. Wright, Kinetics of steady-state currents and charge movements associated with the rat Na^+/glucose cotransporter, J. Biol. Chem. 270 (1995) 27099–27105.
[38] E.M. Wright, D.D. Loo, E. Turk, B.A. Hirayama, Sodium cotransporters, Curr. Opin. Cell Biol. 8 (1996) 468–473.
[39] H. Jung, S. Tebbe, R. Schmid, K. Jung, Unidirectional reconstitution and characterization of purified Na^+/proline transporter of *Escherichia coli*, Biochemistry 37 (1998) 11083–11088.
[40] I. Yamato, Y. Anraku, Alkali Cation Transport Systems in Prokaryotes, CRC Press, Inc, 1993.
[41] K. Hanada, I. Yamato, Y. Anraku, Solubilization and reconstitution of proline carrier in *Escherichia coli*; quantitative analysis and optimal conditions, Biochim. Biophys. Acta 939 (1988) 282–288.
[42] I.C. West, P. Mitchell, Proton/sodium ion antiport in *Escherichia coli*, Biochem. J. 144 (1974) 87–90.
[43] C.L. Brett, M. Donowitz, R. Rao, Evolutionary origins of eukaryotic sodium/proton exchangers, Am. J. Physiol., Cell Physiol. 288 (2005) C223–239.
[44] D. Taglicht, E. Padan, S. Schuldiner, Proton-sodium stoichiometry of NhaA, an electrogenic antiporter from *Escherichia coli*, J. Biol. Chem. 268 (1993) 5382–5387.
[45] E. Padan, T.A. Krulwich, Sodium stress, In: G. Stortz, R. Hengge-Aronis (Eds.), Bacterial Stress Responses, ASM Press, Washington, DC, 2000, pp. 117–130.
[46] E. Padan, S. Schuldiner, Bacterial Na^+/H^+ antiporters — molecular biology, biochemistry and physiology, In: W.N. Konings, H.R. Kaback, J. Lolkema (Eds.), The Handbook of Biological Physics, vol. II, Elsevier Science, Amsterdam, 1996, pp. 501–531.
[47] E. Padan, M. Venturi, Y. Gerchman, N. Dover, Na(+)/H(+) antiporters, Biochim. Biophys. Acta 1505 (2001) 144–157.
[48] M. Venturi, E. Padan, Purification of NhaA Na^+/H^+ antiporter of *Escherichia coli* for 3D and 2D crystallization, In: C. Hunte, G. Von Jagow, H. Schagger (Eds.), A Practical Guide to Membrane Protein Purification, Academic Press, Amsterdam, 2002, pp. 179–190.
[49] E. Padan, T. Tzubery, K. Herz, L. Kozachkov, L. Galili, NhaA of *Escherichia coli,* as a model of a pH regulated Na^+/H^+ antiporter, Biochim. Biophys. Acta 1658 (2004) 2–13.
[50] L. Counillon, J. Pouyssegur, The expanding family of eucaryotic Na(+)/H(+) exchangers, J. Biol. Chem. 275 (2000) 1–4.
[51] J. Orlowski, S. Grinstein, Diversity of the mammalian sodium/proton exchanger SLC9 gene family, Pflugers Arch. 447 (2004) 549–565.
[52] S. Wakabayashi, T. Pang, T. Hisamitsu, M. Shigekawa, The Sodium–Hydrogen Exchange, from Molecule to its Role in Disease, Kluwer Academic Publishers, Boston, 2003.
[53] D. Taglicht, E. Padan, S. Schuldiner, Overproduction and purification of a functional Na^+/H^+ antiporter coded by nhaA (ant) from *Escherichia coli*, J. Biol. Chem. 266 (1991) 11289–11294.
[54] E. Screpanti, C. Hunte, Discontinuous membrane helices in transport proteins and their correlation with function, J. Struct. Biol. 159 (2007) 261–267.
[55] E. Padan, M. Venturi, H. Michel, C. Hunte, Production and characterization of monoclonal antibodies directed against native epitopes of NhaA, the Na^+/H^+ antiporter of *Escherichia coli*, FEBS Lett. 441 (1998) 53–58.
[56] E. Olkhova, C. Hunte, E. Screpanti, E. Padan, H. Michel, Multiconformation continuum electrostatics analysis of the NhaA Na^+/H^+ antiporter of *Escherichia coli* with functional implications, Proc. Natl. Acad. Sci. U. S. A. 103 (2006) 2629–2634.
[57] D. Herzlinger, P. Viitanen, N. Carrasco, H.R. Kaback, Monoclonal antibodies against the lac carrier protein from *Escherichia coli*. 2. Binding studies with membrane vesicles and proteoliposomes reconstituted with purified lac carrier protein, Biochemistry 23 (1984) 3688–3693.
[58] J.L. Rigaud, B. Pitard, D. Levy, Reconstitution of membrane proteins into liposomes: application to energy-transducing membrane proteins, Biochim. Biophys. Acta 1231 (1995) 223–246.
[59] B.A. Hirayama, D.D. Loo, E.M. Wright, Cation effects on protein conformation and transport in the Na^+/glucose cotransporter, J. Biol. Chem. 272 (1997) 2110–2115.